Photonic Crystal Fiber Beamformer for Multiple X-Band Phased-Array Antenna Transmissions

Maggie Yihong Chen, *Member, IEEE*, Harish Subbaraman, and Ray T. Chen, *Fellow, IEEE*

***Abstract*—A multiple-beam optical beamformer based on highly dispersive photonic crystal fibers (PCFs) is presented. Each radio-frequency (RF) beam can be independently controlled to steer continuously. The dispersion of the fabricated PCFs is as high as -600 ps/nm $\cdot$ km at 1550 nm. Simultaneous two-beam transmission is demonstrated using two lasers with different optical wavelengths. The two wavelengths generate two independent sets of time delays, which correspond to two independent RF beams.**

***Index Terms*—Dispersion, optical beamforming, phased-array antenna (PAA), photonic crystal fiber (PCF), true-time delay (TTD).**

I. Introduction

THE high-performance phased-array antenna (PAA) system has been viewed as a technology for the new millennium. Much of the research focus has been on antenna and electronic phase-shifter development. However, ultrawide bandwidth is not available by employing traditional electrical feeding networks due to their intrinsic narrowband nature. Many optical schemes have been proposed to take advantage of a photonic feed for true-time delay (TTD), including bulky optics techniques [1], the dispersive fiber technique [2], the fiber grating technique [3], and substrate guided wave techniques [4]. Multiple radio-frequency (RF) beam beamformers have also been demonstrated utilizing optical TTD by other groups [5]–[8].

In this letter, we report the working principle of a photonic-crystal-fiber (PCF)-based TTD module with multiple beamforming capability for a phased array antenna. The same architecture can also be used as multiple RF beam receivers, which will be published in a separate paper. Compared to the previous work [6], our beamformer utilizes a shorter length of fiber to achieve the same steering angle. The length of the fiber used in reference [6] is 55 m, while our length is 10.5 m. This not only makes the system more compact, but also reduces the overall weight of the system. This can be a very critical requirement when thousands of antenna elements are present in a practical antenna array. Furthermore, since we have the freedom to control the dispersion coefficient in a PCF, much higher values of dispersion can be achieved, reducing the overall length and weight of the system, which is not possible if standard fibers are used.

Manuscript received August 17, 2007; revised December 10, 2007. This work was supported by the Defense Advanced Research Projects Agency (DARPA) under Contract W31P4Q-05-C-0208.

M. Y. Chen is with Omega Optics, Inc., Austin, TX 78758 USA (e-mail: maggie.chen@omegaoptics.com).

H. Subbaraman and R. T. Chen are with the University of Texas at Austin, Austin, TX 78758 USA (e-mail: raychen@uts.cc.utexas.edu).

Color versions of one or more of the figures in this letter are available online at http://ieeexplore.ieee.org.

Digital Object Identifier 10.1109/LPT.2008.916907

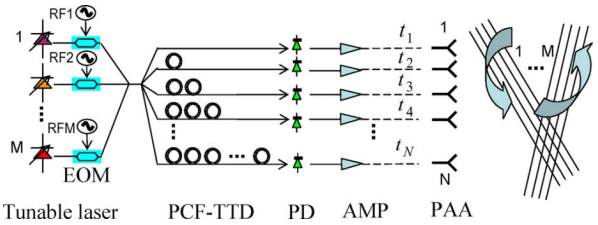

Fig. 1. Multibeam transmitter architecture. PD: photodetector; AMP: amplifier.

II. Multibeam Transmitting PAA

Simultaneous steering of multiple RF beams is very attractive for both military and commercial applications. Multiple-beam transmit/receive functions can be realized by allocating multiple wavelengths. Each wavelength represents a specific RF beam direction. Fig. 1 shows a schematic drawing of the operation principle for optical beamformer architecture with an arbitrary number (M) of wavelengths feeding an N-element array antenna. For a single RF beam generation, only one tunable laser is presented to provide optical carrier with wavelength λ_1. Then it will be modulated with RF signals using an electrooptic modulator (EOM). The modulated optical carrier feeds the PCF-based TTD module. The TTD module is to provide time delay for N-element PAA such that the steering angle can be continuously tuned by tuning the wavelength of the laser. After the pre-designated time delay within the delay modules, the N optical signals are converted into the corresponding electrical signals by N photodetectors as depicted in Fig. 1. The electrical signals are then fed to the N-element phased array antenna head.

The feeding links of each antenna element in Fig. 1 are calibrated to have the same nominal group delay at wavelength λ_0. When the optical wavelength is tuned from λ_0 to λ_1, the time delay t_i corresponding to the ith element of the PAA is expressed as

$$t_i = L_i \cdot \int_{\lambda_0}^{\lambda_1} D(\lambda) d\lambda, \qquad i = 1, \ldots, N \tag{1}$$

where L_i is the length of PCF of the ith delay line, and $D(\lambda)$ is the dispersion value of PCF at optical wavelength λ. The length difference of PCFs between adjacent delay lines are designed as $\Delta L = L_i - L_{i-1}$. Consequently, the time delay interval Δt between adjacent delay lines is

$$\Delta t = \Delta L \cdot \int_{\lambda_0}^{\lambda_1} D(\lambda) d\lambda. \tag{2}$$

The achievable steering angle for the RF beam is

$$\theta = \arcsin\left(\frac{c \cdot \Delta L \cdot \int_{\lambda_0}^{\lambda_1} D(\lambda)d\lambda}{d}\right) \tag{3}$$

where d is the separation between adjacent antenna array elements. It is obvious from the above equation that the beam can be steered by the optical wavelength continuously.

In order to achieve multiple-beam independent operation, we simply need to employ multiple tunable lasers corresponding to the number of beams. In Fig. 1, totally M tunable lasers are employed to generate M independently steered RF beams. Optical carriers from multiple tunable lasers are combined by a $1 \times M$ combiner and simultaneously modulated by an EOM. The modulated optical signals pass through a $1 \times N$ optical power splitter. Then, the optical signals are injected into the PCF-based TTD module, which provides the time delay matrix shown at the bottom of the page, where N is the element number and M is the RF beam number to be independently steered simultaneously. The first row in the matrix represents a time interval $\Delta L \cdot \int_{\lambda_0}^{\lambda_1} D(\lambda)d\lambda$, corresponding to steering angle at $\theta_1 = \arcsin(c \cdot \Delta L \cdot \int_{\lambda_0}^{\lambda_1} D(\lambda)d\lambda/d)$. The second row in the matrix represents a time interval $\Delta L \cdot \int_{\lambda_0}^{\lambda_2} D(\lambda)d\lambda$, corresponding to steering angle at $\theta_2 = \arcsin(c \cdot \Delta L \cdot \int_{\lambda_0}^{\lambda_2} D(\lambda)d\lambda/d)$, while the Mth row in the matrix represents a time interval $\Delta L \cdot \int_{\lambda_0}^{\lambda_M} D(\lambda)d\lambda$, corresponding to steering angle at $\theta_M = \arcsin(c \cdot \Delta L \cdot \int_{\lambda_0}^{\lambda_M} D(\lambda)d\lambda/d)$. The multiple-beam transmitter can continuously steer multiple RF beams with only N delay lines.

III. Continuous Steering of RF Beams

System measurements are performed using the configuration in Fig. 1. The X-band RF signal comes from an 8510C HP network analyzer. The PCF used in the experiment has an experimental dispersion value of -600 ps/nm/km at 1550 nm [9], [10]. With this PCF, the needed dispersion fiber length is reduced six times compare to telecomm dispersion-compensation fibers. The 1545-nm wavelength is chosen as a reference for zero time delay. By tuning the wavelength from 1528 to 1560 nm, time delays ranging from -31.3 to 31.3 ps between any two adjacent delay lines are achieved. This is equivalent to scanning angles from $-45°$ to 45° for a four-element PAA subarray having 1.3-cm spacing, which is the case of our array. We measure the time delay from each delay line at 1550 nm with 1545 nm as the reference using a digital communication analyzer, which is shown in Fig. 2. It is measured that 11.04-ps delay interval is achieved with 5-nm wavelength deviation, which agrees with calculated delay value from the measured dispersion curve [9], [10].

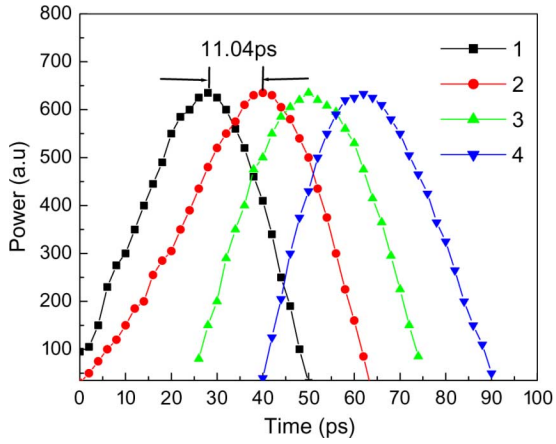

Fig. 2. Measured time delay of four PCF delay lines at 1550 nm.

After the time delay values are measured and confirmed, the continuous steering of one RF beam is demonstrated with the tuning of the optical wavelength. The tunable laser has an output power of 10 dBm. A 2-dB loss is encountered after passing through the EOM. For a 1×4 array, the optical carrier is split into four paths, which creates 6-dB fanout loss for each path. After the optical signals pass through the PCF-TTD line, another 3.2-dB insertion loss is added. Therefore, the total optical loss for each TTD path is 11.2 dB. After the RF signals are detected by photodetectors, a stage of RF amplifiers amplify the RF signals with a saturation power of 5 dBm. At the final stage, the RF signals are fed into a 1×4 X-band array for transmitting.

Fig. 3 shows the experimental results of RF beam steering controlled by optical wavelengths with the dispersion value as a reference. By tuning the wavelength from 1528 to 1560 nm, the RF beam is steered from $-45°$ to 45°.

IV. Multiple-Beam Operation

Two-beam transmission is demonstrated using the configuration in Fig. 1 with two tunable lasers and a four-element PAA. Output RF powers of both beams are measured simultaneously using microwave spectrum analyzer. The 1545-nm wavelength is again chosen as a reference for zero time delay.

Simultaneous transmit beam far field patterns at 8.4 and 12 GHz, together with the theoretical curves (solid line for 8.4 GHz, dashed line for 12 GHz) are shown in Fig. 4. Refering

$$t_{t,k} = \begin{array}{c} \\ 1 \\ 2 \\ . \\ . \\ M \\ \text{(Beam number)} \end{array} \begin{array}{cccc} 1 & 2 & \ldots\ldots & N\text{(element number)} \\ L_1 \cdot \int_{\lambda_0}^{\lambda_1} D(\lambda)d\lambda & L_2 \cdot \int_{\lambda_0}^{\lambda_1} D(\lambda)d\lambda & \ldots & L_N \cdot \int_{\lambda_0}^{\lambda_1} D(\lambda)d\lambda \\ L_1 \cdot \int_{\lambda_0}^{\lambda_2} D(\lambda)d\lambda & L_2 \cdot \int_{\lambda_0}^{\lambda_2} D(\lambda)d\lambda & \ldots & L_N \cdot \int_{\lambda_0}^{\lambda_2} D(\lambda)d\lambda \\ & & & \\ & & & \\ L_1 \cdot \int_{\lambda_0}^{\lambda_M} D(\lambda)d\lambda & L_2 \cdot \int_{\lambda_0}^{\lambda_M} D(\lambda)d\lambda & \ldots & L_N \cdot \int_{\lambda_0}^{\lambda_M} D(\lambda)d\lambda \end{array}$$

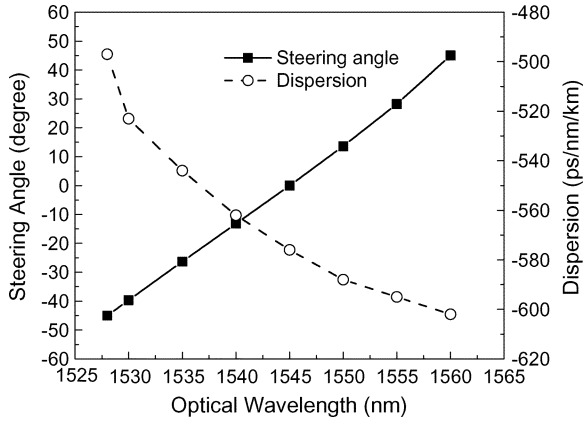

Fig. 3. Experimental results of beam steering versus optical wavelengths, with the dispersion value as a reference.

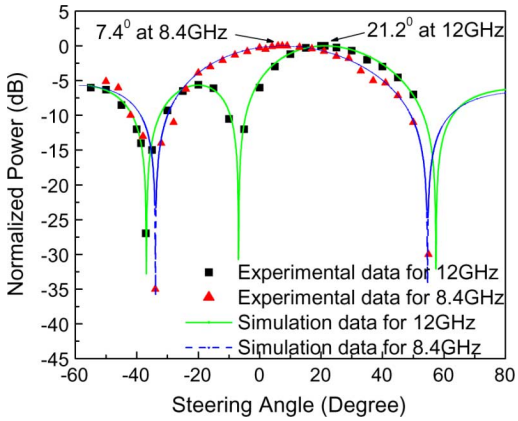

Fig. 4. Simultaneous beam patterns at $+7.4°$ (8.4 GHz) and $+21.2°$ (12 GHz).

to Fig. 3, the optical carrier at 1547.21 nm generates beam steering at $+7.4°$, and the optical carrier at 1552.42 nm generates beam steering at $+21.2°$. To illustrate the performance of the multiple-RF beam beamformer, we need to have multiple wavelengths carrying the signatures of different angles as implied in Fig. 3. Simultaneously steering two angles is demonstrated for the first time using highly dispersive PCFs. Fig. 5 shows the experimental results of the far field patterns of two close RF center frequencies. The carrier optical wavelengths are 1547.21 and 1553.02 nm corresponding to $+7.4°$ and $+23°$ steering referring to Fig. 3. Fig. 5 shows the theoretical and experimental far field patterns of two-beam at $+7.4°$ at 8.3 GHz and $+23°$ at 8.4 GHz. The experimental results of two-beam simultaneously steering agree very well with theoretical curves.

V. Conclusion

We present a multiple-beam optical beamformer based on highly dispersive PCFs. The TTD beamformer can be programmed to continuously sweep the antenna aperture independently for multiple RF beams. Two-beam transmission is demonstrated by using two carriers with different optical

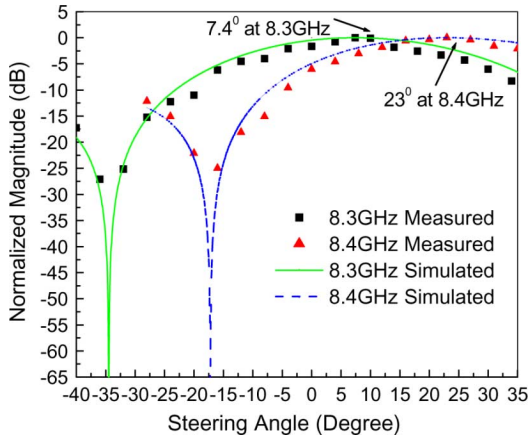

Fig. 5. Simultaneous beam patterns at $+7.4°$ (8.3 GHz) and $+23°$ (8.4 GHz).

wavelengths, which generate two independent sets of time delays. Since the dispersion of the fabricated PCFs employed is as high as -600 ps/nm $\cdot$ km at 1550 nm, the length of delay line is reduced by six times compared to telecom dispersion compensation fiber with -100 ps/nm $\cdot$ km, which reduces the weight and size of the TTD beamformer correspondingly.

Acknowledgment

The authors would like to thank S. Pappert, R. Esman, and G. Brost for their support in various stages of the program.

References

[1] N. A. Riza, "Liquid crystal-based optical time delay units for phased array antennas," *J. Lightw. Technol.*, vol. 12, no. 8, pp. 1440–1447, Aug. 1994.

[2] R. D. Esman, M. Y. Frankel, J. L. Dexter, L. Goldberg, M. G. Parent, D. Stilwell, and D. G. Cooper, "Fiber-optic prism true time-delay antenna feed," *IEEE Photon. Technol. Lett.*, vol. 5, no. 11, pp. 1347–1349, Nov. 1993.

[3] A. Molony, C. Edge, and I. Bennion, "Fibre grating time delay element for phased array antennas," *Electron. Lett.*, vol. 31, no. 17, pp. 1485–1486, Aug. 1995.

[4] Y. Chen and R. T. Chen, "A fully packaged true time delay module for a k-band phased array antenna system demonstration," *IEEE Photon. Technol. Lett.*, vol. 14, no. 8, pp. 1175–1177, Aug. 2002.

[5] N. A. Riza, "An acoustooptic-phased-array antenna beamformer for multiple simultaneous beam generation," *IEEE Photon. Technol. Lett.*, vol. 4, no. 7, pp. 807–809, Jul. 1992.

[6] P. J. Matthews, M. Y. Frankel, and R. D. Esman, "A wideband fiber-optic true-time-steered array receiver capable of multiple independent simultaneous beams," *IEEE Photon. Technol. Lett.*, vol. 10, no. 5, pp. 722–724, May 1998.

[7] S. Granieri, M. Jaeger, and A. Siahmakoun, "Multiple-beam fiber-optic beamformer with binary array of delay lines," *J. Lightw. Technol.*, vol. 21, no. 12, pp. 3262–3272, Dec. 2003.

[8] N. A. Riza, "High speed multi-beamforming for wideband phased arrays," in *IEEE Int. Topical Meeting Microwave Photonics*, 2003, pp. 405–409.

[9] Y. Jiang, B. Howley, Z. Shi, Q. Zhou, R. Chen, M. Chen, G. Brost, and C. Lee, "Dispersion-enhanced photonic crystal fiber array for a true time delay structured X-band phased array antenna," *IEEE Photon. Technol. Lett.*, vol. 17, no. 1, pp. 187–189, Jan. 2005.

[10] Y. Jiang, Z. Shi, B. Howley, X. Chen, M. Y. Chen, and R. T. Chen, "Delay time enhanced photonic crystal fiber array for wireless communications using 2-D X-band phased-array antennas," *Opt. Eng.*, vol. 44, p. 125001, 2005.